Experimental Eye Research 243 (2024) 109890

Contents lists available at ScienceDirect

Experimental Eye Research

journal homepage: www.elsevier.com/locate/yexer

Research article

Possible retinotoxicity of long-term vardenafil treatment

Klaudia Szabó [a,b,1], Bulcsú Dékány [b,1], Anna Énzsöly [b,c], Rozina Ida Hajdú [b,c,d], Lenke Kornélia Laurik-Feuerstein [c], Arnold Szabó [b], Tamás Radovits [e], Csaba Mátyás [e], Attila Oláh [e], Krisztián András Kovács [f], Ágoston Szél [b], Gábor Márk Somfai [c,g,h], Ákos Lukáts [f,b,*]

[a] Institute of Education and Psychology at Szombathely, Faculty of Education and Psychology, ELTE Eötvös Loránd University, Szombathely, Hungary
[b] Department of Anatomy, Histology and Embryology, Semmelweis University, Budapest, Hungary
[c] Department of Ophthalmology, Semmelweis University, Budapest, Hungary
[d] Eye Center, Medical Center, Faculty of Medicine, University of Freiburg, Freiburg, Germany
[e] Heart and Vascular Center, Semmelweis University, Budapest, Hungary
[f] Institute of Translational Medicine, Translational Retina Research Group, Semmelweis University, Budapest, Hungary
[g] Spross Research Institute, Zurich, Switzerland
[h] Department of Ophthalmology, Stadtspital Zurich, Zurich, Switzerland

ARTICLE INFO

Keywords:
Retina
Photoreceptors
Type 2 diabetes mellitus
Vardenafil
Retinotoxicity

ABSTRACT

Phosphodiesterase (PDE) inhibitors – such as vardenafil – are used primarily for treating erectile dysfunction via increasing cyclic guanosine monophosphate (cGMP) levels. Recent studies have also demonstrated their significant cardioprotective effects in several diseases, including diabetes, upon long-term, continuous application. However, PDE inhibitors are not specific for PDE5 and also inhibit the retinal isoform. A sustained rise in cGMP in photoreceptors is known to be toxic; therefore, we hypothesized that long-term vardenafil treatment might result in retinotoxicity. The hypothesis was tested in a clinically relevant animal model of type 2 diabetes mellitus. Histological experiments were performed on lean and diabetic Zucker Diabetic Fatty rats. Half of the animals were treated with vardenafil for six months, and the retinal effects were evaluated. Vardenafil treatment alleviated rod outer segment degeneration but decreased rod numbers in some positions and induced changes in the interphotoreceptor matrix, even in control animals. Vardenafil treatment decreased total retinal thickness in the control and diabetic groups and reduced the number of nuclei in the outer nuclear layer. Müller cell activation was detectable even in the vardenafil-treated control animals, and vardenafil did not improve gliosis in the diabetic group. Vardenafil-treated animals showed complex retinal alterations with improvements in some parameters while deterioration in others. Our results point towards the retinotoxicity of vardenafil, even without diabetes, which raises doubts about the retinal safety of long-term continuous vardenafil administration. This effect needs to be considered when approving PDE inhibitors for alternative indications.

1. Introduction

Diabetes mellitus (DM) and its complications pose an ever-increasing economic and social burden on modern societies. Today, more than 500 million people are estimated to live with this disease, and this number is predicted to rise well above 600 million by 2030 (International Diabetes Federation, 2022). As a chronic disease, long-standing and poorly treated DM damages almost all organ systems with serious, sometimes even life-threatening complications in the kidney (diabetic nephropathy (Qi et al., 2017)), in the cardiovascular system (Strain and Paldánius, 2018) and in the visual system (diabetic retinopathy (Wang and Lo, 2018; Rodríguez et al., 2019; Kang and Yang, 2020)), among others.

A large number of studies conducted over the last decades have helped to increase our understanding of the development of these complications and identified a series of common features in their pathomechanisms, including microvascular alterations (Hammes, 2005; Tomlinson and Gardiner, 2008; Shin et al., 2014), inflammation (Kinuthia et al., 2020), activation of the polyol pathway (Ramadan, 2007) and accumulation of glycated end products (Lorenzi, 2007; Sharma et al., 2012), for example. The accumulating knowledge has led to the identification of several theoretically feasible therapeutic

* Corresponding author. Institute of Translational Medicine, Translational Retina Research Group, Semmelweis University, Budapest, Hungary.
E-mail address: lukatsakos@gmail.com (Á. Lukáts).
[1] Klaudia Szabó and Bulcsú Dékány have contributed equally to this work and are considered first authors.

https://doi.org/10.1016/j.exer.2024.109890
Received 11 July 2023; Received in revised form 10 March 2024; Accepted 9 April 2024
Available online 13 April 2024

Abbreviations

AO	Anti-rhodopsin
ARVO	The Association for Research in Vision and Ophthalmology
cGMP	Cyclic guanosine monophosphate
DAPI	4,6-diamidino-2-phenylindole
DM	Diabetes mellitus
GFAP	Glial fibrillary acidic protein
ILM	Inner limiting membrane
IPM	Interphotoreceptor matrix
M-cones	Middle wavelength sensitive cones
NeuN	Neuron-specific nuclear protein
NO	Nitric oxide
OLM	Outer limiting membrane
ONL	Outer nuclear layer
PAH	Pulmonary arterial hypertension
PB	Phosphate buffer
PDE	Phosphodiesterase
PNA	Peanut agglutinin lectin
RPE	Retinal pigment epithelium
RPE-65	Retinal pigment epithelium-specific 65 kDa protein
SD	Standard deviation
sGC	soluble guanylate cyclase
T2D	Type 2 diabetes
TUNEL	Terminal deoxynucleotidyl transferase deoxyuridine triphosphate nick end labeling
ZDF	Zucker Diabetic Fatty

approaches – besides the normalization of blood glucose levels - to slow down disease progression and the development of its complications (Oshitari, 2021; Ala et al., 2020). Some of these new therapies have undergone preclinical testing and are currently in the clinical trial phase; some are already in regular use as approved therapies (Gross et al., 2018).

One of the most severe challenges in the therapy of diabetes is the diverse clinical manifestations of the disease, with almost all organs affected. Drugs that have a beneficial effect on one organ system may have adverse effects on others. In the case of drugs with systemic effects or administered systematically, i.e. when organ-specific delivery is not possible, this may be a crucial issue to consider.

The phosphodiesterase (PDE) inhibitors (such as sildenafil or vardenafil) and guanylate cyclase activators/stimulators (cinaciguat or riociguat, for example) have recently been demonstrated to exert cardioprotective effects in several cardiovascular diseases, including ischemia-reperfusion injury or diabetic cardiomyopathy (Mátyás et al., 2015, 2018; Korkmaz-Icöz et al., 2018; Veres et al., 2018; Benke et al., 2020). Long-term application of vardenafil successfully prevented the development of heart failure with preserved ejection fraction in both type 1 and type 2 diabetic rat models (Radovits et al., 2009; Mátyás et al., 2017). Existing PDE5 inhibitors, however, are known to be non-specific, with measurable inhibitory effects on the retinal PDE6 enzyme as well (Zhang et al., 2005; Cote, 2004). Side effects, such as vision deterioration, color vision problems (red desaturation), and perception of increased brightness of light, have been regularly reported in a dose-dependent manner (Marmor and Kessler, 1999) when these drugs were administered for erectile dysfunction – with a cumulative dose of just a fraction of what is lately being proposed against diabetes. Although existing toxicology studies claim that these side effects are temporary and fully reversible (Marmor and Kessler, 1999; Abbott et al., 2004) extreme elevation of cGMP levels in photoreceptor cells is known to be toxic: abnormally high cGMP concentrations and decreased PDE6 function or a decline in PDE6 expression are responsible for some forms of retinitis pigmentosa and are present in rd1 and rd10 mouse models (Azevedo et al., 2014; Kalloniatis et al., 2016; Wang et al., 2018). Therefore, we hypothesized, that long-term, continuous vardenafil treatment could result in detectable retinotoxicity. Correspondingly, preclinical and clinical studies need to be extended to longer, continuous dosing regimens before PDE5 inhibitors are approved for alternative indications by regulatory authorities.

For the above reasons, the present study aimed to investigate the potential retinotoxic effects of the PDE5 inhibitor vardenafil in Zucker Diabetic Fatty (ZDF) rats in a long-term application at a clinically relevant dose already shown to exert significant cardioprotective effects (Mátyás et al., 2017). Results were compared with previously published histological findings of diabetic retinal alterations in the same type 2 diabetic (T2D) rat model (Szabó et al., 2017).

2. Materials and methods

2.1. Animal model and tissue preparation

All procedures were performed in concordance with the Association for Research in Vision and Ophthalmology (ARVO) statement for the Use of Animals in Ophthalmic and Vision Research. The study was approved by the local Ethics Committee for Animal Experimentation of Semmelweis University and by the Animal Health and Animal Welfare Directorate of the National Food Chain Safety Office of the Hungarian State (number of approval: January 22, 1162/3/2010).

ZDF inbred, male rats were obtained from Charles River Laboratories (Sulzfeld, Germany). In ZDF rats, T2D and related complications develop due to a leptin receptor gene mutation and a special diet. Homozygous recessive males develop obesity, fasting hyperglycemia, and T2D (referred to below as "ZDF diabetic"). Homozygous dominant and heterozygous genotypes remain normoglycemic ("ZDF lean"). Details about animal handling and diabetes control were given elsewhere (Mátyás et al., 2018; Szabó et al., 2017). In brief, animals were delivered at the age of 6 weeks and were randomly divided into four groups: vehicle-treated controls (ZDF lean; n = 8), vehicle-treated diabetic (ZDF diabetic; n = 8), vardenafil-treated controls (ZDF lean + vardenafil; n = 7) and vardenafil-treated diabetic (ZDF diabetic + vardenafil; n = 7). Animals received *per os* drug treatment (10 mg/kg body weight vardenafil dissolved in 0.01 mol/L citrate buffer) or vehicle (0.01 mol/L citrate buffer) from the 7th week of age. The body weights of the animals were measured on every second day, and the dose of vardenafil was adjusted accordingly. Blood glucose levels were measured regularly with a digital blood glucose meter (Accu-Chek® Sensor; Roche, Mannheim, Germany).

At the age of 32 weeks, anesthesia was induced, and after a series of cardiovascular examinations and hemodynamic measurements (including echocardiography, left ventricular pressure–volume analysis, cardiomyocyte force measurements, detailed in Mátyás et al., 2017, 2018) the animals were euthanized by exsanguination and decapitated. The eyes were removed, the eyecups were dissected and placed into fixative (4 % paraformaldehyde diluted in 0.1 M phosphate buffer [PB, pH 7.4] for 2 h at room temperature). After cryoprotection (30 % sucrose diluted in 0.1 M PB), the eyecups were embedded in a tissue-embedding medium (Shandon Cryomatrix, Thermo Scientific, UK) and frozen in custom made blocks on the surface of an aluminum cube cooled down by immersing into liquid nitrogen. 20 μm thick cryosections were cut vertically and stored at −20 °C until use.

2.2. Immunohistochemistry

Detailed descriptions of the immunolabeling protocol have already been published in our previous studies (Szabó et al., 2017; Énzsöly et al.,

2014). Primary antibodies (with their details listed in Table 1) were all applied overnight at 4 °C. Bound antibodies were visualized by species-specific fluorescent probes (Alexa 488 or Alexa 594 conjugates, 1:200, Life Technologies, Carlsbad, CA) applied for 2 h at room temperature. Cell nuclei were counterstained with DAPI (4,6-diamidino-2-phenylindole, Sigma-Aldrich Kft, Budapest, Hungary). Sections with the primary antibodies omitted were used as negative controls. All antibodies applied have been tested and validated in ZDF rat retinae previously (Szabó et al., 2017; Hajdú et al., 2019).

Peanut agglutinin lectin (PNA) was applied in a biotinylated form (2 h - detailed in Table 1) and was detected with streptavidin-linked Alexa dies (1:200, Life Technologies, Carlsbad, CA).

2.3. Imaging

A Zeiss LSM 780 Confocal System coupled to a Zeiss Axio Imager upright microscope, a 40x objective (NA = 1,4) and Zen 2012 software (Carl Zeiss, Oberkochen, Germany) was used for image recording. Care was taken to use strictly identical settings for each group. The final montages were created and labeling was added by Adobe Photoshop 7.0 (San Diego, CA, USA).

2.4. Measurement of retinal thickness

Retinal thickness measurements were performed according to previously published protocols (Szabó et al., 2017) at six defined locations (250 and 500 μm (central values), as well as 4000 μm (peripheral values) from the optic nerve head in both superior and inferior directions), on four sections per each retina and on four specimens from each group. The distance between the outer and inner limiting membranes (OLM-ILM) and the thickness of the outer nuclear layer (ONL) was measured on vimentin-stained slides, where the proper plane of the sectioning could be easily confirmed. Additionally, the number of nuclei in the ONL columns was counted parallel to the thickness measurements. Only vertical cryosections at the level of the optic nerve were analyzed using a Zeiss Axiophot (Carl Zeiss, Oberkochen, Germany) microscope with a 40x (NA: 1,4) oil immersion objective.

2.5. Apoptosis and counting immunolabeled cells

Apoptotic cells were visualized using the terminal deoxynucleotidyl transferase deoxyuridine triphosphate nick end labeling (TUNEL, *In situ* Cell Death Detection Kit, Fluorescein; Roche Diagnostics, Mannheim, Germany) assay following the manufacturer's instructions. For negative controls, we used sections without the terminal transferase enzyme, while positive control sections were pre-incubated with DNAse I prior to performing the TUNEL reaction.

Counting immunolabeled microglia cells and ganglion cells, as well as TUNEL positive elements, was performed on complete 20 μm thick vertical sections (4 sections per specimen) taken from 4 different animals from each group. Only the sections going through the optic nerve head were selected; sections taken from the same specimen were approximately 100 μm away from each other in the temporo-nasal direction. M-cones (middle wavelength sensitive cones) were counted on images reconstructed from confocal stacks, using 15 μm thickness and 425 μm long region of the section. Counting was performed in central (immediately adjacent to the optic nerve head), mid-peripheral (approximately 3 microscopical visual fields – 875 μm away from the optic disc), and peripheral (approximately 6 visual fields – 1925 μm away from the optic nerve) regions in both superior and inferior directions. Data was collected from 4 animals from each group, 4 sections were analyzed from each specimen.

The same images were also used to quantify M-cone outer segment degeneration, but only central retinal regions were examined in details. All cones with signs of outer segment degeneration were identified, counted and the results were expressed as percentage of M-cones.

2.6. Quantifying müller glia activation

The extent of glial activation was quantified by measuring the length of the activated areas of each section and dividing it by the total length of the same section. A Zeiss Axiophot (Carl Zeiss, Oberkochen, Germany) microscope with a 20x objective was used for quantification, which was performed on 4 sections per specimen from 4 different animals per group. The results were presented as a percentage of the glial fibrillary acidic protein (GFAP) activation. The advantage of this method is that it

Table 1
The list of the primary antibodies used in the study.

Antibodies (name, clone and cat. number)	Source	Working concentration	Host and type	Epitope specificity or labelling pattern in rats	Reference
Iba1, Clone: #019-19741	Wako Chemicals Inc, USA	1:500	rabbit polyclonal	microglia cells	Roger et al., 2012; Szabó et al. (2017)
GFAP, Clone: G-A-5, #G-3893	Sigma-Aldrich Kft., Budapest, Hungary	1:1000	mouse monoclonal	astrocytes and Müller cells in retinal injuries	Szabó et al. (2017); Lieth et al. (1998)
vimentin, Clone: V-9, #MAB3400	Millipore, Billerica, MA, USA	1:10000	mouse monoclonal	Müller cells	Fernández-Sánchez et al. (2015)
NeuN, Clone: A60, #MAB377	Merck Kft., Budapest, Hungary	1:100	mouse monoclonal	ganglion cells and some amacrine cells	Hajdú et al. (2019); Zeng et al. (2000)
Brn-3a, #SC-31984	Santa Cruz Biotechnology, Inc., Heidelberg, Germany	1:500	goat polyclonal	ganglion cells	Hajdú et al. (2019); Charalambous et al. (2013)
OS-2	produced in the laboratory of Pál Röhlich and Ágoston Szél	1:5000	mouse monoclonal	S-cone opsin, S-cones	Szabó et al. (2017); Röhlich and Szél (1993)
Rb X opsin red/green, #AB5405	Millipore, Billerica, MA	1:1000	rabbit polyclonal	M-cone opsin, M-cones	Szabó et al. (2017); Ng et al. (2011)
AO	produced in the laboratory of Pál Röhlich and Ágoston Szél	1:100	rat polyclonal	rhodopsin, rod photoreceptors	Szabó et al. (2017); Röhlich and Szél (1993)
RPE-65, Clone: #MAB5428	Merck Kft., Budapest, Hungary	1:500	mouse monoclonal	isomerohydrolase (retinal pigment epithelium)	Szabó et al. (2017); Susaki et al. (2009)
cone arrestin, Clone: #AB15282	Millipore, Billerica, MA	1:1000	rabbit polyclonal	cone photoreceptors	Szabó et al. (2017); McGill et al. (2012)
PNA, Clone: #L6135	Sigma-Aldrich Kft., Budapest, Hungary	5 mg/ml	lectin, binding to galactosyl-β(1,3)- N-acetyl-D-galactosamine residues	interphotoreceptor matrix of cones, IPL sublayers	Hageman and Johnson (1986)

GFAP: glial fibrillary acidic protein, NeuN: neuron-specific nuclear protein, AO: anti-rhodopsin, PNA: peanut agglutinin lectin, RPE-65: retinal pigment epithelium-specific 65 kDa protein.

is normalized for the length of the section, and comparison can be made between sections (eyes) that may be different in size.

2.7. Statistical analysis

All data are presented as mean ± standard deviation (SD). For statistical comparison of the groups in case of blood glucose levels and the weights of the animals, two-way ANOVA test was used with the Bonferroni post hoc test (N = 7 or 8 animals from each group). For comparing other parameters derived from lower number of animals (N = 4 - retinal thickness analysis, TUNEL, gliosis and microglia activation, cone number and morphology and ganglion cell numbers) data from each animal (obtained from the quantification of 4 sections per specimen) was averaged and presented as a single value. Group average was calculated from 4 animals and compared by Kruskal-Wallis test with Dunn's post hoc test. In all cases, a p value less than 0.05 was deemed to be significant.

3. Results

A detailed description of the retinal alterations in untreated diabetic ZDF rats compared with lean counterparts has already been published (Szabó et al., 2017). However, to allow a better understanding of the effects of vardenafil, we recite these results here and also present some representative pictures from untreated animals.

3.1. Body weights and fasting blood glucose levels

The time-course of body weight and blood glucose level changes of diabetic ZDF rats and lean controls were similar to those published by the supplier (Charles River Laboratories, Sulzfeld, Germany) and have already been published in detail elsewhere (Szabó et al., 2017). In brief: no significant difference in average body weights was detectable at the time of anesthesia (421.3 ± 26.1 g in lean and 400.3 ± 50.2 g in diabetic animals, p = 0.81). Vardenafil treatment did not cause any significant change in the body weights of the animals, neither in the lean nor in the diabetic groups, although some tendency of decrease in weights was visible in both cases. The average body weight in the lean + vardenafil group was: 411.1 ± 28.9 g (p = 0.97 lean vs. lean + vardenafil) and 385.8 + 62.9 g in the diabetic + vardenafil group (p = 0.92 diabetic vs. diabetic + vardenafil).

Blood glucose levels were already elevated at the 7th week and remained significantly higher in all diabetic animals throughout the entire observation period compared with controls. No difference was visible in blood glucose levels between treated and untreated groups at any time examined, indicating that the retinal effects of vardenafil

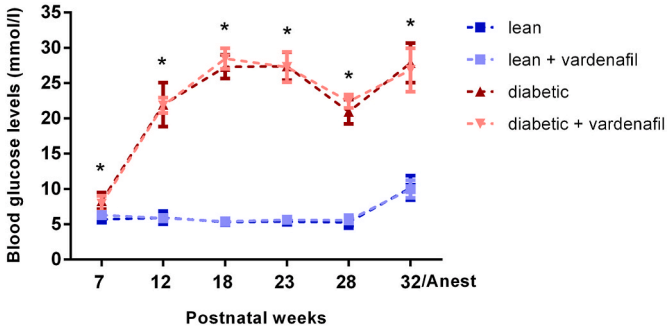

Fig. 1. Blood glucose levels in lean and diabetic ZDF rats with and without vardenafil treatment. Based on statistical analysis, blood glucose levels were significantly higher in untreated diabetic animals compared with the untreated lean group from the 7th postnatal week till the 32nd week (time of anesthesia). Vardenafil treatment had no effect on glucose levels neither in lean, nor in diabetic animals. *: p < 0.05 lean vs. diabetic.

treatment, if detectable, were not related to changes in glucose homeostasis (Fig. 1). Details of the statistical analysis, along with the appropriate p values are given in the Supplementary materials (Table S1).

3.2. Retinal thickness and apoptosis rates

In a previous report we have already reported a significant increase in total retinal thickness (OLM-ILM distance) in diabetic ZDF rats compared with lean specimens (Szabó et al., 2017). With non-parametric test, the increase was significant only in one retinal position. This increase was most probably the result of edema formation. Vardenafil application in general decreased retinal thickness both in the diabetic and in the lean groups compared with the respective untreated groups (Fig. 2a). The difference was statistically significant in all positions except the middle superior and inferior peripheral retina in diabetic specimens. In the case of lean rats, significant difference was detectable only in the inferior central position.

Similarly to total retinal thickness, ONL thickness was also significantly higher in diabetic specimens compared with the lean group in all inferior and in the superior peripheral positions examined (Szabó et al., 2017). Vardenafil treatment did not cause any significant change in ONL thickness compared with the appropriate untreated groups (Fig. 2b).

The decreased retinal thickness after vardenafil treatment observed in both groups could potentially be explained by assuming 1) either changes in the extra- or intracellular fluid content and/or alternatively 2) by cell loss due to neurotoxicity. To examine this latter possibility, we estimated the number of several cell types and performed a quantitative TUNEL labeling.

Rods constitute about 70% of all retinal cells in rodents (Carter--Dawson and Lavail, 1979). Their number can be estimated by counting their nuclei. In well-oriented radial sections, the nuclei in the ONL are arranged in discernible columns, and their number in each column can be counted relatively easily, as done by our group and others in previous reports (Szabó et al., 2017; Di Pierdomenico et al., 2018; Starr et al., 2019; Xie et al., 2020). Summarized results are shown in Fig. 2c. While there was no difference detectable between untreated diabetic and lean specimens in the average number of cells in the ONL columns, vardenafil treatment caused a significant decrease in cell numbers in some positions tested. This effect of vardenafil could be demonstrated in both groups when compared with their appropriate controls. Changes were detected in the superior central and peripheral positions in the case of lean and inferior central and peripheral positions in diabetic specimens after vardenafil treatment. Details of the statistical analysis for total retinal thickness, ONL thickness, and number of nuclei in the ONL columns, along with the appropriate p values, are given in the Supplementary materials (Tables S2–4). Images demonstrating the above-mentioned changes in retinal thickness are shown in Fig. 4 (a-d and e-h). Results of cone- and ganglion cell number estimations will be presented in the relevant sections below.

To further examine a possible loss of cells, TUNEL reactions were performed on a set of radial sections but did not reveal any differences between lean and diabetic specimens (lean 4.06 ± 1.41 elements/section vs diabetic 2.63 ± 1.48 elements/section, p = 0.89). Furthermore, no significant difference was detectable between treated and untreated animals, neither in the lean nor in the diabetic groups (lean 4.06 ± 1.41 elements/section vs lean + vardenafil 5.23 ± 1.66 elements/section (p = 0.83 lean vs lean + vardenafil) and diabetic 2.63 ± 1.48 elements/section vs diabetic + vardenafil: 5.00 ± 0.84 elements/section (p = 0.17 diabetic vs diabetic + vardenafil)) (Fig. 3).

3.3. Glial response

Müller glia activation was examined by GFAP immunoreactions. In lean ZDF rats, in line with literature data (Lieth et al., 1998), GFAP immunoreactivity was confined to the end feet of Müller glia cells and

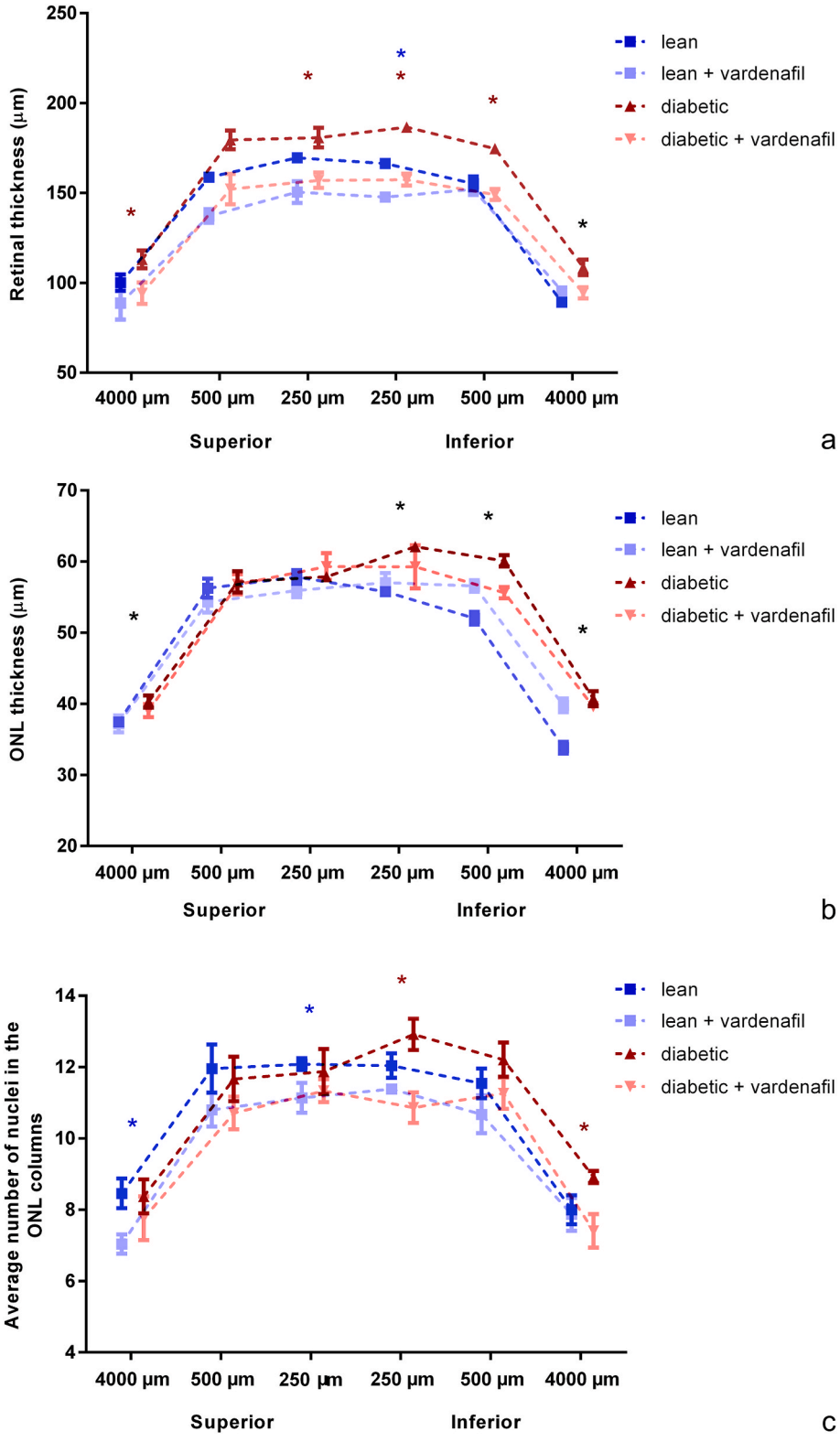

(caption on next page)

astrocytes of the nerve fiber layer for the majority of the retina (Fig. 4a). The radial processes of Müller cells showed labeling only in the extreme peripheral retina (7.86% ± 1.63% of the complete retinal section lengths) (Szabó et al., 2017) (Fig. 4i). In contrast to this, in diabetic rats Müller cells were heavily labeled by GFAP over the complete retina (Fig. 4b–i). The quantified difference in GFAP labeled areas between lean and diabetic groups was significant. Vardenafil treatment did not affect the GFAP labeling pattern in diabetic specimens (Fig. 4d) but resulted in evident glial activation in the lean group (Fig. 4c–i). Unlike in untreated lean animals, radial Müller cell labeling appeared in central

Fig. 2. Retinal thickness (a), outer nuclear layer (ONL) thickness (b), and number of nuclei in the ONL columns (c) in control and diabetic ZDF rats with and without vardenafil treatment. Samples were taken 250 μm, 500 μm, and 4000 μm superiorly and inferiorly from the optic nerve head. Total retinal thickness (a) was significantly elevated in one position in diabetic specimens compared with lean counterparts (black *, $p < 0.05$). Vardenafil treatment decreased retinal thickness in general, which was significant in lean specimens in the inferior central position (blue *, $p < 0.05$). In vardenafil-treated diabetic specimens retinal thickness decreased significantly in all retinal positions except the middle superior and the inferior peripheral regions compared with diabetic untreated specimens (red *, $p < 0.05$). ONL thickness (b) was significantly higher in all inferior and in the superior peripheral retinal positions in diabetic specimens compared with leans (black *, $p < 0.05$). Vardenafil treatment had no further significant effect on the values detected. The photoreceptor nuclei in the ONL are arranged in discernible columns. Counting the number of nuclei in these columns (c) demonstrated no significant difference between lean and diabetic specimens. Vardenafil treatment significantly decreased the number of nuclei in the columns in two superior regions in lean specimens (blue *, $p < 0.05$) and in the inferior central and peripheral positions in the diabetic animal groups (red *, $p < 0.05$). ONL: outer nuclear layer. (For interpretation of the references to color in this figure legend, the reader is referred to the Web version of this article.)

retinal regions as well, in approximately 50% of the entire retinal length (48.94 ± 11.12%, Fig. 4i) in vardenafil-treated lean specimens. Despite this evident change in GFAP staining pattern, the quantification of the percentage of labeled areas with non-parametric test failed to reveal any significant difference between the lean vardenafil-treated group compared with all other groups (Fig. 4i).

Vimentin is another intermediate filament found in Müller cells. Our previous report revealed no difference in the labeling pattern or intensity between lean and diabetic specimens (Szabó et al., 2017). Fig. 4g and h shows representative images from vardenafil-treated animals. Here there was no detectable difference between lean and diabetic animals, either.

An increase in the number of microglia cells has been shown to occur in diabetic ZDF rats (Szabó et al., 2017) (Fig. 5a and b). Quantification of the results of Iba-1 labeling (Fig. 5e) also demonstrated a significant increase in the number of microglia cells in diabetic untreated specimens compared with untreated controls (lean: 82.50 ± 3.35 cells/section vs diabetic: 218.30 ± 58.38 cells/section, $p = 0.01$). Vardenafil treatment alone does not cause microglia activation in lean rats (lean: 82.50 ± 3.35 cells/section vs lean + vardenafil: 91.14 ± 20.18 cells/section, $p > 0.99$, Fig. 5c), but decreases the number of detectable microglia cells in diabetic specimens (diabetic: 218.30 ± 58.38 cells/section vs diabetic + vardenafil: 149.81 ± 34.02 cells/section), however, with non-parametric test, this difference was not significant $p > 0.99$, Fig. 5d).

3.4. Photoreceptor cell response

In diabetic ZDF rats, a prominent outer segment degeneration was detectable for the majority of rods and M-cones without an evident decrease in the number of photoreceptor cells (Fig. 6) (Szabó et al., 2017). This phenomenon was also detected in other diabetic models and has previously been examined in detail by both light and electron microscopy (Szabó et al., 2017; Énzsöly et al., 2014; Hammoum et al., 2017). Interestingly, vardenafil treatment seemingly improved rod outer segment morphology (Fig. 6a–d) but had no visible effect on the degeneration of M-cone outer segments (Fig. 6e–h). Quantification for M-cone degeneration revealed a significant difference in the percentage of cone outer segments showing signs of degeneration (incomplete fragmentation) between lean and diabetic specimens (lean 12.51 ± 3.59% vs. diabetic 94.46 ± 2.08%; $p = 0.04$). Vardenafil treatment had no effect on this value, neither in lean (lean + vardenafil 14.23 ± 1.55%; $p > 0.99$ lean vs lean + vardenafil) nor in diabetic specimens (diabetic + vardenafil 95.11 ± 2.46%; $p > 0.99$ diabetic vs diabetic + vardenafil). Regarding the number of labeled elements, no significant difference was detected in M-cone numbers in the treated groups compared with untreated ones (Fig. 6i). Details of the statistical analysis, along with the appropriate p values are given in the Supplementary materials (Table S5).

Rod numbers were only indirectly estimated by measuring ONL thickness and the number of nuclei in the ONL columns. As discussed in detail previously, vardenafil had no effect on ONL thickness, but caused a significant decrease in the number of nuclei in some but not all positions, suggesting a possible decrease in rod numbers (Fig. 2c).

Photoreceptor maintenance and function strongly depends on the well-being of the retinal pigmented epithelium (RPE) (Strauss, 2005). To examine RPE pathology, the cells were labeled by an antibody against an RPE-specific enzyme isomerohydrolase (RPE-65), that exhibited a prominent decrease in staining intensity in diabetic specimens, irrespectively of vardenafil treatment (Fig. 6a–d).

Cone morphology and interphotoreceptor matrix (IPM) labelling was further examined by a cone arrestin antibody and PNA labeling. No change in staining intensity or pattern was detectable with the cone arrestin antibody in diabetic ZDF rats when compared with lean counterparts, but evident outer segment degeneration was visible in diabetic animals (Fig. 7a and b) (Szabó et al., 2017). Vardenafil treated groups showed no alterations compared with the respective untreated groups. Furthermore, unlike in the case of rods, cone outer segment morphology did not improve in diabetic rats after vardenafil treatment (Fig. 7c and d).

There was no detectable difference in PNA staining pattern between untreated lean and diabetic ZDF rats (Fig. 7e and f) (Szabó et al., 2017). However, importantly, vardenafil treatment triggered a conspicuous change in PNA staining. PNA lectin started to label a small number of rods besides cones in the non-diabetic animals exposed to vardenafil, and produced an intensive and well visible rod and cone labeling in vardenafil-treated diabetic animals, indicating a change in the glycosylation of the IPM components (Fig. 7g and h). Representative images from a total of 16 animals (that is from all of the 4 animals from all of the 4 groups) demonstrate (Supplementary Fig. S1) that the above-mentioned alterations were present in all specimens examined. Co-labeling with cone arrestin and PNA were also used to prove that some PNA positive elements in the photoreceptor layer – the ones that were cone arrestin negative - were undoubtedly rods (Supplementary Fig. S2).

3.5. Ganglion cell response

Ganglion cells were labeled on cryosections using the Neu-N and Brn-3a antibodies. No change was detected in the staining pattern or intensity or in the number of stained elements between lean and diabetic specimens (Fig. 8a and b), in line with our previous publications (Szabó et al., 2017; Hajdú et al., 2019). Similarly, vardenafil treatment had no effect on staining intensity (Fig. 8c and d) or ganglion cell numbers (lean: 318.9 ± 16.89 cells/section, lean + vardenafil: 333.69 ± 21.45 cells/section, diabetic: 347.6 ± 14.13 cells/section, diabetic + vardenafil: 343.50 ± 7.91 cells/section, $p = 0.09$ for lean vs. diabetic, $p = 0.90$ for lean vs. lean + vardenafil, and $p > 0.99$ for diabetic vs. diabetic + vardenafil, Fig. 8e).

4. Discussion

Long-lasting diabetes mellitus often leads to compromised function of almost all organ systems, including the kidney, the central as well as peripheral nervous systems, and the cardiovascular system (Feldman et al., 2019; Qi et al., 2017; Strain and Paldánius, 2018; Wang and Lo, 2018; Rodríguez et al., 2019; Kang and Yang, 2020). The impairment of the crucial functions of these organs, like the appearance of diabetic

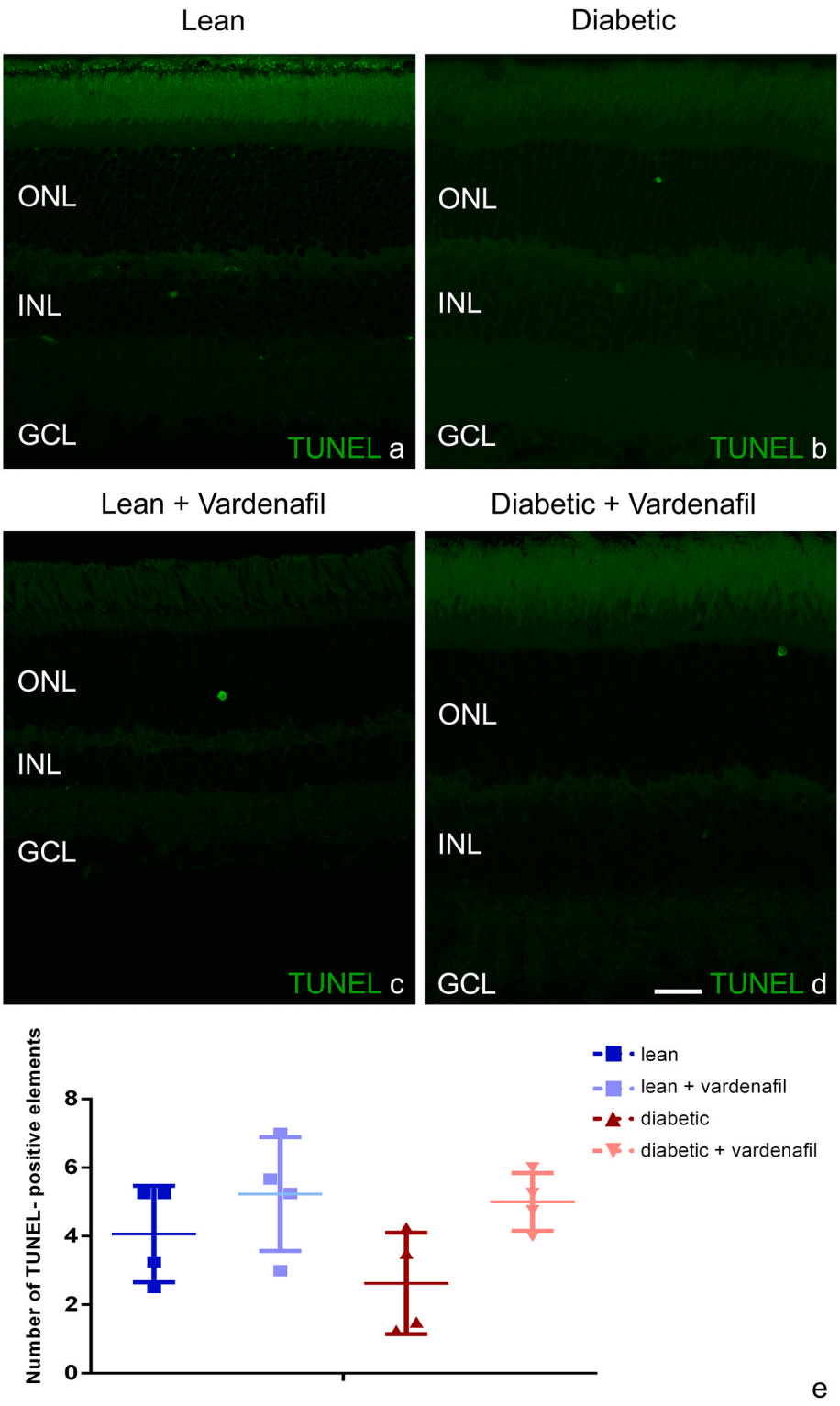

Fig. 3. TUNEL-positive elements in lean and diabetic ZDF rats with and without vardenafil treatment. Representative images demonstrate TUNEL-positive elements in the ONL in lean (a), diabetic (b), and vardenafil-treated lean and diabetic groups (c and d, respectively). Labeling was quantified in all retinal layers in complete retinal sections from 4 animals per group, on 4 sections from each animal. Statistical analysis (e) of the number of TUNEL-positive elements per section revealed no significant difference between the groups tested. ONL: outer nuclear layer, INL: inner nuclear layer, GCL: ganglion cell layer. *Bar*: 20 μm.

cardiomyopathy characterized by decreased cardiac function and endothelial cell dysfunction – can initiate a vicious circle, thereby further worsening the conditions of diabetic patients (Viigimaa et al., 2020). Deteriorating circulation increases hypoxia and decreases nutrient supply all around the body, contributing to kidney dysfunction (Qi et al., 2017) and the development of nervous system pathologies (Iribarne and Masai, 2017), among others. Therefore, it is logical to assume that any therapy improving cardiovascular health of diabetic patients will have a beneficial effect on other compromised organ systems. That may indeed be the case for most therapeutic approaches as

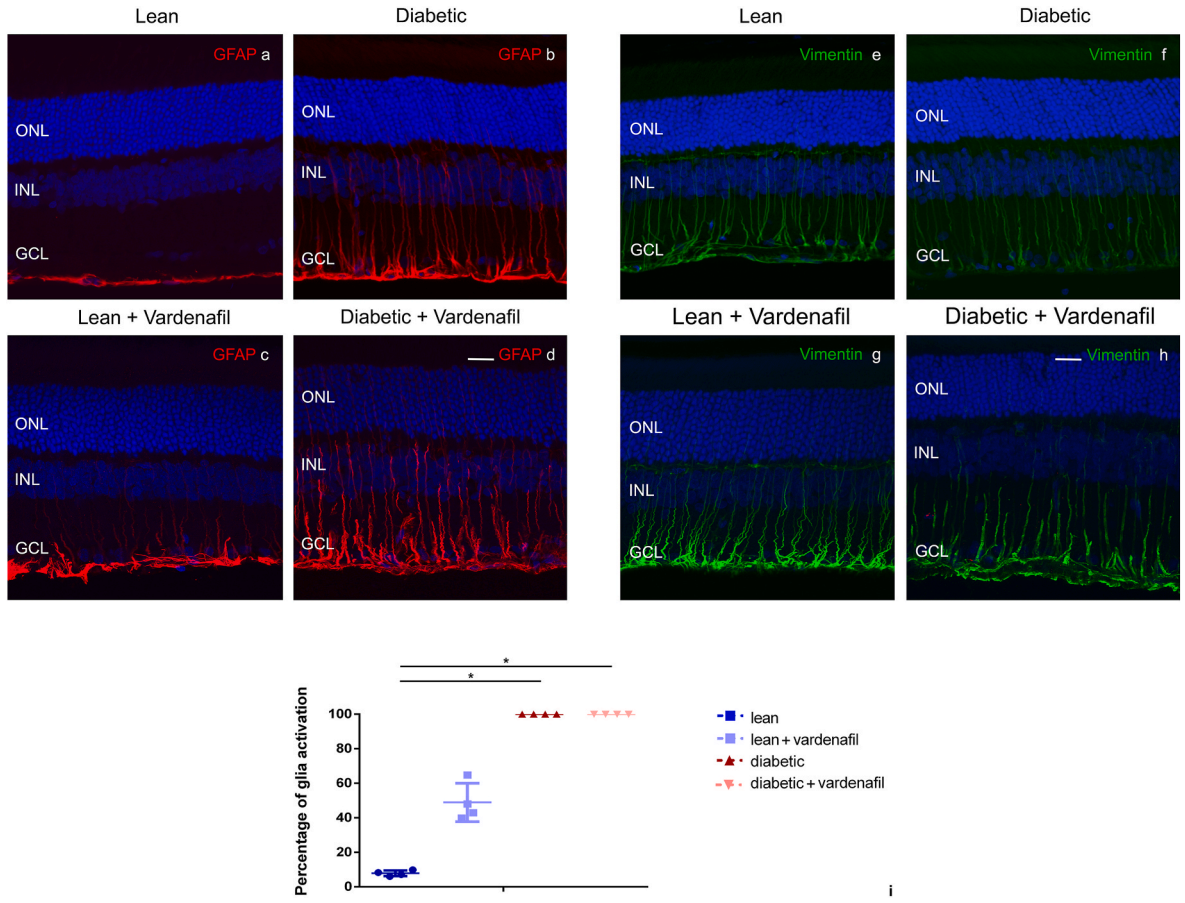

Fig. 4. Glial response in lean and diabetic ZDF rats with and without vardenafil treatment. GFAP labeling (a-d, in red) in lean rats was restricted to the inner retina (inner limiting membrane and astrocytes of the nerve fiber layer); Müller cell bodies were labeled only in the extreme peripheral retina. In vardenafil-treated lean ZDF rats, GFAP labeling appeared in Müller cell processes in some retinal parts in the central retina, as well (c). In diabetic rats, strong GFAP activation was detectable all over the retina, both in vardenafil-treated (d) and untreated specimens (b). Vimentin labeling of Müller glia cells (e-h, in green) demonstrated no evident difference between lean (e) and diabetic (f) animals. Vardenafil treatment also did not affect labeling pattern or intensity (g-h, lean and diabetic, respectively). DAPI is used for orientation (in blue). Quantified results of Müller cell activation (expressed as the percentage of retinal section length with prominent GFAP labeling) are summarized in Fig. 4i. While in lean untreated specimens, GFAP labeling was restricted to a small percentage of the retina, in diabetic animals, the complete retinal length exhibited strong GFAP staining with 100% of the retina being labeled in all sections and in all specimens examined, both in the treated and untreated groups. Interestingly, vardenafil treatment alone induced Müller glia activation in lean specimens, however the quantified rate of this activation did not reach the level of statistically significance. ONL: outer nuclear layer, INL: inner nuclear layer, GCL: ganglion cell layer. *: $p < 0.05$. *Bar*: 20 μm. (For interpretation of the references to color in this figure legend, the reader is referred to the Web version of this article.)

long as these do not have organ-specific side effects elsewhere in the body.

Based on the observed involvement of the nitrogen monoxide-cGMP axis in diabetic cardiomyopathy, PDE5 inhibitors have emerged as a possible therapeutic choice in diabetes. Indeed, recently published reports claimed that long-term, continuous vardenafil treatment can successfully prevent the development of cardiovascular dysfunction in rat models of both type 1 (Radovits et al., 2009) and type 2 diabetes mellitus (ZDF rats (Mátyás et al., 2017)). Administered in a daily dose of 10 mg/kg, vardenafil treatment elevated cGMP levels and significantly improved cardiac function, contractility, and vasorelaxation in both models. Vardenafil thus seems to have favorable effects in diabetes, at least as far as circulation is concerned.

However, most of the PDE5 inhibitors available to date (including sildenafil and vardenafil) are not absolutely specific for the PDE5 subtype: they also inhibit PDE6, found in photoreceptors of the retina, causing an elevation of cGMP inside these cells as well (Zhang et al., 2005; Iribarne and Masai, 2017; Campbell and Jensen, 2017). cGMP is the intracellular messenger of the rods and cones of the retina, playing a crucial role in visual signal transduction. Inhibiting the retinal PDE6, the degradation of cGMP is deteriorated resulting in high cGMP levels, which may affect adversely the photoreceptor function and – in the case of a long-term application – it may even be toxic for rods and cones (Azevedo et al., 2014; Kalloniatis et al., 2016; Wang et al., 2018).

The main indication today for taking PDE5 inhibitors, such as sildenafil and vardenafil, is male erectile dysfunction, when a single dose daily is recommended, with 20 mg vardenafil or 100 mg sildenafil not to be exceeded. Retinal side effects, most probably associated with increased cGMP levels, are frequently documented and appear to be dose-dependent. These include transitory visual disturbances, a blue tinge to vision, and increased brightness perception, with concomitant alterations of the electroretinogram also reported (Roessler et al., 2019). These ocular side effects are believed to be reversible; furthermore, available toxicity studies did not report any signs of degeneration even after long-term application of PDE5 inhibitors (Ala et al., 2020).

However, in the case of existing or suggested alternative indications, such as pulmonary arterial hypertension (PAH) or diabetic cardiomyopathy, much larger daily cumulative doses should be administered to reach the desired effect on the circulatory system. In the case of PAH - an already approved indication in the case of sildenafil - the recommended dosing is 5–20 mg, 4–6 times a day. This may cause a less pronounced but continuous increase in cGMP levels as opposed to the single peak of

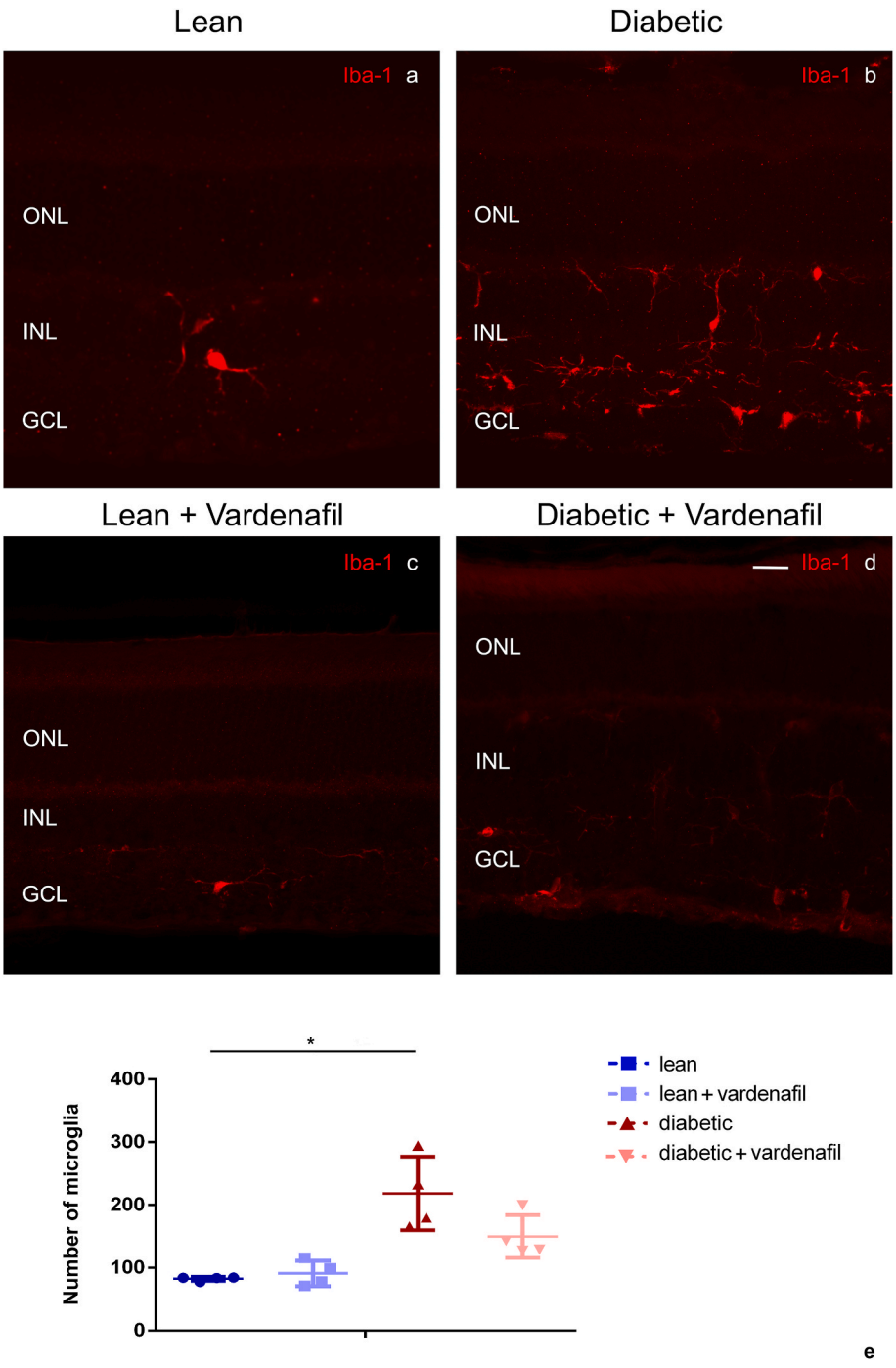

Fig. 5. Microglia cells in lean and diabetic ZDF rats with and without vardenafil treatment. Microglia cells were labeled by Iba-1 antibody. No difference was detectable in microglia cell morphology neither between untreated control (a) and diabetic specimens (b) nor between the vardenafil-treated lean (c) and diabetic groups (d). Quantitative analysis (e) demonstrated significantly increased microglia numbers in untreated diabetic specimens compared with the control group. Vardenafil did not affect microglia numbers in lean specimens but seemingly decreased the numbers in diabetic animals, but this change was not significant. *: $p < 0.05$. ONL: outer nuclear layer, INL: inner nuclear layer, GCL: ganglion cell layer. *Bar*: 20 μm.

the conservative application and thus may affect the retina differently. Consequently, more thorough and detailed retinal toxicity studies are warranted before alternative applications of these drugs make their way to everyday practice.

In our model presented here, diabetic and lean animals were treated daily for 6 months with a relatively high dose of vardenafil. At the age of 32 weeks, the animals were euthanized, and the cardiovascular status (echocardiography, left ventricular pressure–volume analysis, cardiomyocyte force measurements) along with the health of the retinal tissue was assessed. According to previously published data the dose chosen by us here was clinically relevant, as significant improvements in cardiac and renal functions were reported in the same animals (Mátyás et al., 2017) and even in STZ-induced diabetic rats (Radovits et al., 2009; Fang et al., 2013) after the treatment. Furthermore, other studies also used similar dose ranges in rats (Sandner et al., 2015; Alp et al., 2017; Salama et al., 2018; Aziret et al., 2014) and reported favorable results in several disease models.

The retinal effects of long-term vardenafil administration were

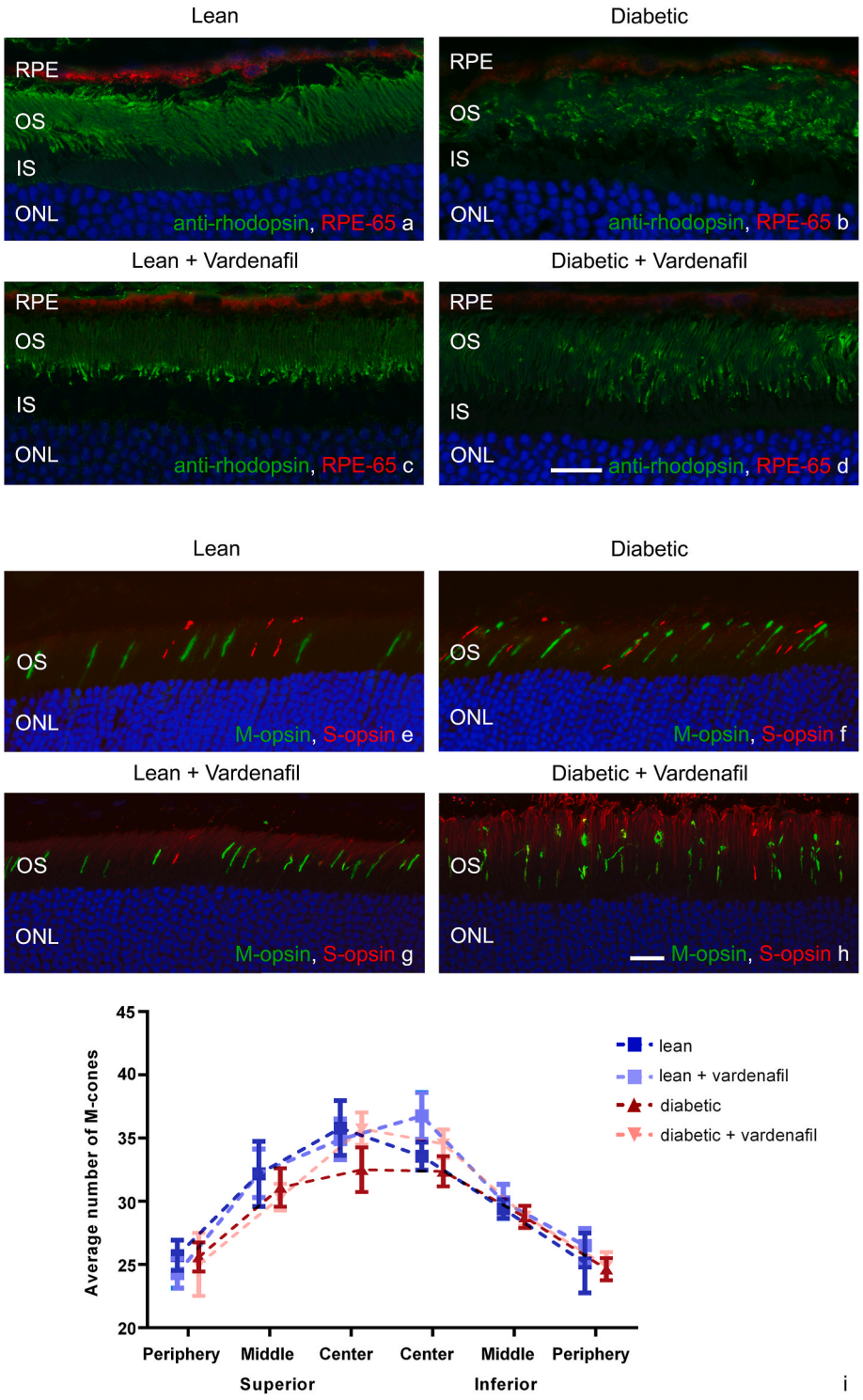

Fig. 6. Photoreceptor pathology in lean and diabetic ZDF rats with and without vardenafil treatment. Rods - labeled by anti-rhodopsin antibody (a-d, in green) - exhibited severe signs of outer segment degeneration in untreated diabetic ZDF rats (b), compared with untreated controls (a). Vardenafil treatment did not affect rod outer segment morphology in controls (c), but the improvement was evident in vardenafil-treated diabetic animals (d). RPE-65 antibody stains the retinal pigment epithelium (a-d, in red). In untreated diabetic animals, a decrease in staining intensity was detectable (b) compared with controls (a). Vardenafil treatment did not significantly affect RPE staining (c, d). Cone subtypes were labeled by M- and S-opsin-specific antibodies (e-h, in green and red, respectively). M-cones also exhibited severely degenerated morphology in untreated diabetic specimens, with partially fragmented outer segment pieces (f). Vardenafil treatment did not influence M-cone morphology in lean animals (g); however, unlike in the case of rods, it did not prevent diabetic damage (h). Statistical analysis revealed no significant difference in M-cone numbers between any of the groups examined (i). There was no evident change in the S-opsin labeling (e-h, in red). DAPI is used for orientation (in blue). RPE: retinal pigment epithelium, OS: outer segments, IS: inner segments, ONL: outer nuclear layer, *Bar*: 20 μm. (For interpretation of the references to color in this figure legend, the reader is referred to the Web version of this article.)

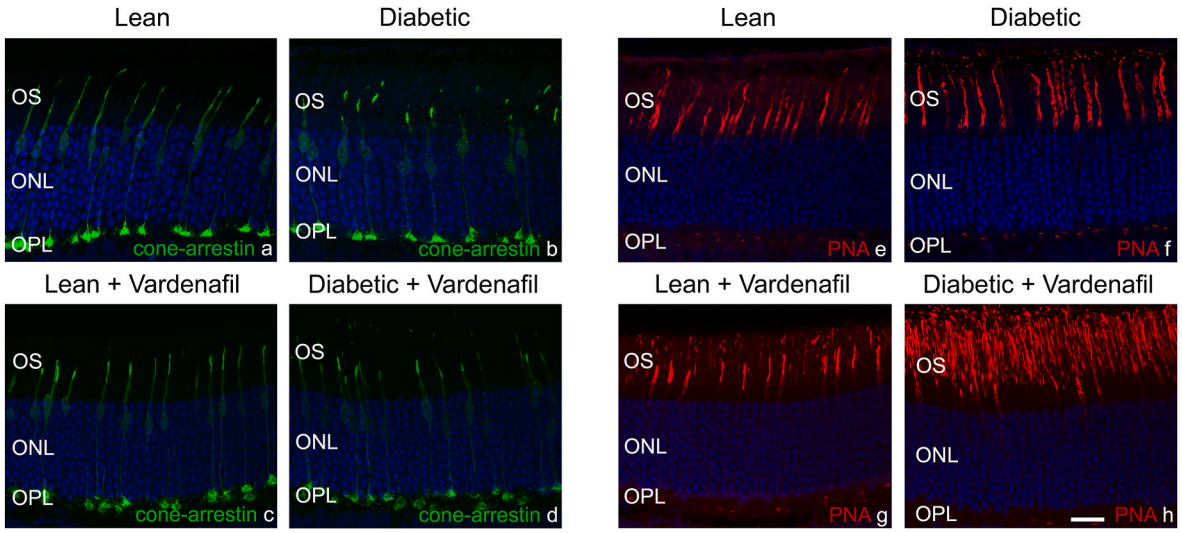

Fig. 7. Cone arrestin and PNA staining in lean and diabetic ZDF rats with and without vardenafil treatment. Cone outer segment degeneration was also evident with cone arrestin staining (a-d, in green) in the diabetic untreated group (b) compared with control (a). Vardenafil treatment did not affect cone outer segment morphology (c, d) compared with the appropriate untreated groups (a, b). PNA lectin normally stains the interphotoreceptor matrix (IPM) of cones (e-h, in red). No evident change was detectable in untreated diabetic specimens (f) compared with untreated controls (e). After vardenafil treatment, PNA signal also appeared in the IPM around rods, even in lean animals (g), and the rod staining became drastically stronger in the vardenafil-treated diabetic group (h). DAPI is used for orientation (in blue). OS: outer segments, ONL: outer nuclear layer, OPL: outer plexiform layer. *Bar*: 20 μm. (For interpretation of the references to color in this figure legend, the reader is referred to the Web version of this article.)

diverse. Improvements were detectable in some parameters, such as microglia activation and rod outer segment morphology. In contrast, other parameters showed evident deterioration (rod numbers and glycosylation of the IPM components) or remained unchanged (cone outer segment morphology, RPE labeling and ganglion cell numbers).

Improvements may be induced either directly by the positive retinal actions of vardenafil or – more probably – indirectly by improving the cardiovascular status. Nitric oxide (NO) plays an important role in the regulation of retinal blood flow (for review see: Wright et al., 2020), so altered NO-sGC-cGMP axis – as present after vardenafil treatment – may increase retinal blood flow. This may be protective, as retinal blood flow is reported to be decreased in early diabetes (Wright et al., 2020). Furthermore, previous reports had shown, that ZDF rats develop diabetic cardiomyopathy - hear failure with preserved ejection fraction – by 32 weeks of age (Mátyás et al., 2017, 2018). This is characterized predominantly by deteriorations in diastolic function, hypertrophy, fibrotic remodeling, with the clinical signs of heart failure, but with preserved left ventricular function. This was successfully prevented in treated animals by long-term vardenafil application, by improving cardiac status which can indirectly improve retinal circulation as well.

Despite and opposing all the possible positive effects, some of the changes detected were clearly suggestive of the possible direct retinotoxicity of the treatment.

Changes in retinal thickness constitute one of the best examples of the opposing actions of the treatment. Total thickness values indicated that the diabetic retinae were actually thicker than the lean counterparts, most probably due to edema formation. Intracellular edema (Tomlinson and Gardiner, 2008) and extracellular fluid accumulation due to increased retinal permeability (Xu et al., 2011) could contribute to this increase. Not surprisingly, therefore, we confirmed that vardenafil treatment decreased retinal thickness values in both diabetic and lean groups. Any contribution of the decreased intracellular edema to this decrease seems unlikely, as no difference in glucose homeostasis was detectable. Positive hemodynamic effects and improving cardiovascular status may partially be responsible for this change; with the caveat that decreased thickness in some positions coincided with a decrease in the number of nuclei in the ONL columns. As this latter is a well-known, and regularly applied estimation of rod numbers in rodents (Szabó et al., 2017; Di Pierdomenico et al., 2018; Starr et al., 2019; Xie et al., 2020) it clearly argues in favor of significant photoreceptor loss.

Interestingly, in this report we did not detect any increase in the number of TUNEL positive elements at the time of euthanasia. This seemingly contradicts major cell loss; however, we must point out, that TUNEL labeling is a far less sensitive method than the quantification of the ONL nuclei, especially if a continuous, but low degree photoreceptor loss is suspected. Compared to TUNEL reactions, that only label the cells undergoing apoptosis precisely at the time of sampling, quantifying the number of nuclei estimates cumulative loss of cells – over a period of 32 weeks in this case. In a study, like this one, where the overall decrease in photoreceptor numbers is in the range of approximately 10%, TUNEL may simply lack sensitivity to detect this. Furthermore, we must point out again, that a significant decrease in rod numbers was evident even in vardenafil-treated lean animals, which clearly indicates the toxicity of this dosing regimen to rods. The fact that a change in the glycosylation of the IPM around rods was detectable after vardenafil treatment also suggests a toxic effect related to the administered molecule. Again, this was visible even in lean specimens.

Overall, these results clearly point towards a potential photoreceptor loss and question the safety of long-term, continuous, high-dose vardenafil administration. Our results indicate that cGMP levels may reach sufficiently high levels to induce photoreceptor damage, similar to what can be seen in some forms of retinitis pigmentosa (Azevedo et al., 2014; Kalloniatis et al., 2016; Wang et al., 2018). This must be considered if non-selective PDE inhibitors are planned to be used for alternative indications in humans. A thorough toxicity study should be performed, and the dosing or the administration should be modified to decrease the unintended retinal side effects. Tadalafil may not have retinal adverse effects being more specific for the PDE5 subtype (Zhang et al., 2005). Alternatively, soluble guanylate cyclase (sGC) activators and stimulators may achieve the same increase in vascular cGMP levels and the same improvement in cardiovascular status (Sandner et al., 2021; Stasch et al., 2011). Although sGC activity is also present in some cells of the inner retina (Vielma et al., 2012), it is absent from photoreceptors; therefore, the retinal safety profile is expected to be superior to PDE5 inhibitors. Further experiments are warranted to examine this possibility.

Some limitations of this study have to be mentioned. First, ZDF rats

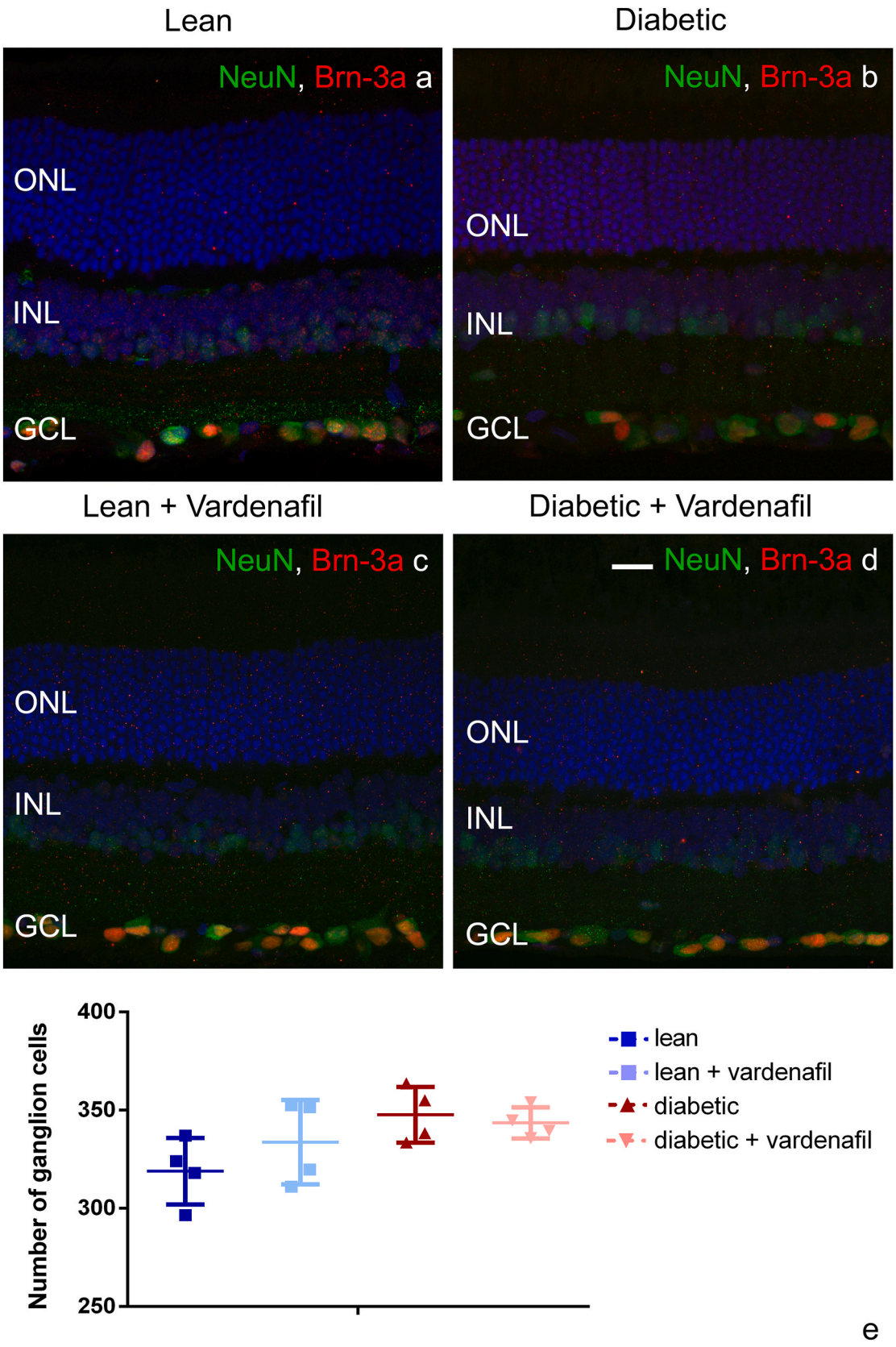

Fig. 8. Ganglion cell staining in vardenafil treated and untreated ZDF diabetic and lean rats. Ganglion cells were labeled with two pan-ganglionic markers, NeuN (a-d, in green) and Brn-3a (a-d, in red). The staining patterns were practically identical in the untreated control (a) and diabetic (b) animals and also after vardenafil treatment (c, d). Quantitative analysis using the Brn-3a antibody demonstrated no significant difference between any of the groups (e). DAPI is used for orientation (in blue). ONL: outer nuclear layer, INL: inner nuclear layer, GCL: ganglion cell layer. *Bar*: 20 μm. (For interpretation of the references to color in this figure legend, the reader is referred to the Web version of this article.)

develop T2D-like alterations due to a leptin receptor mutation. Therefore, the pathomechanism and also some manifestations are inherently different from T2D in human patients (Wang et al., 2014) that must be considered when interpreting the results. Leptin and leptin receptors are known to play roles in neovascularization and angiogenesis (Suganami et al., 2004; Scolaro et al., 2013). Furthermore, leptin levels correlate with some vascular ophthalmic diseases: elevated vitreous levels were detected in proliferative diabetic retinopathy (Maberley et al., 2006; Er et al., 2005), serum levels are elevated in retinal vein occlusion (Ates et al., 2008) and correlate with some vascular parameters (van Aart et al., 2018; Ahiante et al., 2020). Retinal vascular alterations were not examined here and the typical retinal vascular complications of diabetes do not develop in ZDF rats (and also in most other rodent models of diabetes in the time range examined), we can not fully rule out, that the direct vascular effect of leptin receptor mutation was – at least partially – responsible for some of the changes detected.

Furthermore, the dose chosen here as well as in most other studies performed in rats (Radovits et al., 2009; Mátyás et al., 2017; Fang et al., 2013; Sandner et al., 2015; Alp et al., 2017; Salama et al., 2018; Aziret et al., 2014) is higher than those applied or suggested in human patients. This may partially be explained with differences in the metabolic rate and undoubtedly, this higher dose exerts significant protective effect in rats, in several disease models, including, but not limited to cardiovascular pathologies. However, the lack of direct comparability of the doses limits the translational potential of this study, as far as photoreceptor toxicity is concerned. The mere chance, that such toxicity is present in animal models and it is possible in human patients certainly urge for further studies.

5. Conclusions

In summary, we report here that long-term, continuous vardenafil application has prominent toxic effects on the retina, although it does improve the cardiovascular status in models of type 2 diabetes. This phenomenon must be taken into account before such treatment is applied on human patients.

Funding

TKP2021-EGA-23 has been implemented with the support provided by the Ministry of Innovation and Technology of Hungary from the National Research, Development and Innovation Fund, financed under the TKP2021-EGA funding scheme.

Project no. RRF-2.3.1-21-2022-00003 has been implemented with the support provided by the European Union.

CRediT authorship contribution statement

Klaudia Szabó: Writing – original draft, Validation, Methodology, Investigation, Data curation, Conceptualization. **Bulcsú Dékány:** Writing – original draft, Visualization, Methodology, Investigation, Data curation. **Anna Énzsöly:** Methodology, Investigation, Conceptualization. **Rozina Ida Hajdú:** Visualization, Investigation. **Lenke Kornélia Laurik-Feuerstein:** Investigation, Conceptualization. **Arnold Szabó:** Visualization, Validation, Conceptualization. **Tamás Radovits:** Writing – review & editing, Supervision, Funding acquisition, Conceptualization. **Csaba Mátyás:** Methodology, Investigation. **Attila Oláh:** Methodology, Investigation. **Krisztián András Kovács:** Writing – review & editing, Visualization. **Ágoston Szél:** Writing – original draft, Validation, Supervision. **Gábor Márk Somfai:** Writing – review & editing, Writing – original draft, Validation, Supervision, Conceptualization. **Ákos Lukáts:** Writing – review & editing, Writing – original draft, Visualization, Validation, Supervision, Methodology, Data curation, Conceptualization.

Declaration of competing interest

G.M.S. has received speaker and consultant honoraria from Allergan, Bayer, Novartis, Roche and Carl Zeiss Meditec. All other authors (K.Sz., B.D., A.É., R.I.H., L.K.L., A. Sz., T.R., Cs.M., A.O., K.A.K., Á.Sz. and Á.L.) declare no potential conflict of interest.

Data availability

All data used is present in the manuscript and in the Supplementary Information of the manuscript

Acknowledgements

The valuable assistance of Éva Kovácsné Dobozi and the assistants of the Heart and Vascular Center is highly appreciated. The authors would like to thank Pál Röhlich for the critical reading and correction of the manuscript.

Appendix A. Supplementary data

Supplementary data to this article can be found online at https://doi.org/10.1016/j.exer.2024.109890.

References

Abbott, D., Comby, P., Charuel, C., Graepel, P., Hanton, G., Leblanc, B., Lodola, A., Longeart, L., Paulus, G., Peters, C., Stadler, J., 2004. Preclinical safety profile of sildenafil. Int. J. Impot. Res. 16, 498–504. https://doi.org/10.1038/sj.ijir.3901232.

Ahiante, B.O., Smith, W., Lammertyn, L., Schutte, A.E., 2020. Leptin and the retinal microvasculature in young black and white adults: the african-PREDICT study. Heart Lung Circ. 29, 1823–1831. https://doi.org/10.1016/j.hlc.2020.05.093.

Ala, M., Jafari, R.M., Dehpour, A.R., 2020. Sildenafil beyond erectile dysfunction and pulmonary arterial hypertension: thinking about new indications. Fundam. Clin. Pharmacol. 35, 235–259. https://doi.org/10.1111/fcp.12633.

Alp, H.H., Huyut, Z., Yildirim, S., Başbugan, Y., Ediz, L., Şekeroğlu, M.R., 2017. The effect of PDE5 inhibitors on bone and oxidative damage in ovariectomy-induced osteoporosis. Exp. Biol. Med. Maywood. 242, 1051–1061. https://doi.org/10.1177/1535370217703352.

Ates, O., Keles, M., Bilen, H., Kiziltunc, A., Kocer, I., Kulacoglu, D.N., Türkeli, M., Baykal, O., 2008. Increased serum levels of leptin in retinal vein occlusion. Tohoku J. Exp. Med. 215, 373–376. https://doi.org/10.1620/tjem.215.373.

Azevedo, M.F., Faucz, F.R., Bimpaki, E., Horvath, A., Levy, I., de Alexandre, R.B., Ahmad, F., Manganiello, V., Stratakis, C.A., 2014. Clinical and molecular genetics of the phosphodiesterases (PDEs). Endocr. Rev. 35, 195–233. https://doi.org/10.1210/er.2013-1053.

Aziret, M., Irkorucu, O., Reyhan, E., Erdem, H., Das, K., Ozkara, S., Surmelioglu, A., Sozen, S., Bali, I., Cetinkunar, S., Deger, K.C., 2014. The effects of vardenafil and pentoxifylline administration in an animal model of ischemic colitis. Clinics 69, 763–769. https://doi.org/10.6061/clinics/2014(11)10.

Benke, K., Németh, B.T., Sayour, A.A., Stark, K.A., Oláh, A., Ruppert, M., Szabó, G., Korkmaz-Icöz, S., Horváth, E.M., Benkő, R., Hartyánszky, I., Szabolcs, Z., Merkely, B., Radovits, T., 2020. Stimulation of soluble guanylate cyclase improves donor organ function in rat heart transplantation. Sci. Rep. 10, 5358. https://doi.org/10.1038/s41598-020-62156-y.

Campbell, L.J., Jensen, A.M., 2017. Phosphodiesterase inhibitors sildenafil and vardenafil reduce zebrafish rod photoreceptor outer segment shedding. Invest. Ophthalmol. Vis. Sci. 58, 5604–5615. https://doi.org/10.1167/iovs.17-21958.

Carter-Dawson, L.D., Lavail, M.M., 1979. Rods and cones in the mouse retina. I. Structural analysis using light and electron microscopy. J. Comp. Neurol. 188, 245–262. https://doi.org/10.1002/cne.901880204.

Charalambous, P., Wang, X., Thanos, S., Schober, A., Unsicker, K., 2013. Regulation and effects of GDF-15 in the retina following optic nerve crush. Cell Tissue Res. 353, 1–8. https://doi.org/10.1007/s00441-013-1634-6.

Cote, R.H., 2004. Characteristics of photoreceptor PDE (PDE6): similarities and differences to PDE5. Int. J. Impot. Res. 1, 28–33. https://doi.org/10.1038/sj.ijir.3901212.

Di Pierdomenico, J., Scholz, R., Valiente-Soriano, J., Sánchez-Migallón, M.C., Vidal-Sanz, M., Langmann, T., Agudo-Barriuso, M., García-Avuso, D., Villegas-Pérez, M.P., 2018. Neuroprotective effects of FGF2 and minocycline in two animal models of inherited retinal degeneration. Invest. Ophthalmol. Vis. Sci. 59, 4392–4403. https://doi.org/10.1167/iovs.18-24621.

Énzsöly, A., Szabó, A., Kántor, O., Dávid, C., Szalay, P., Szabó, K., Szél, Á., Németh, J., Lukáts, Á., 2014. Pathologic alterations of the outer retina in streptozotocin-induced diabetes. Invest. Ophthalmol. Vis. Sci. 55, 3686–3699. https://doi.org/10.1167/iovs.13-13562.

Er, H., Doğanay, S., Ozerol, E., Yürekli, M., 2005. Adrenomedullin and leptin levels in diabetic retinopathy and retinal diseases. Ophthalmologica 219, 107–111, 1159/000083270.

Fang, L., Radovits, T., Szabó, G., Mózes, M.M., Rosivall, L., Kökény, G., 2013. Selective phosphodiesterase-5 (PDE-5) inhibitor vardenafil ameliorates renal damage in type 1 diabetic rats by restoring cyclic 3',5' guanosine monophosphate (cGMP) level in podocytes. Nephrol. Dial. Transplant. 28, 1751–1761. https://doi.org/10.1093/ndt/gfs391.

Feldman, E.L., Callaghan, B.C., Pop-Busui, R., Zochodne, D.W., Wright, D.E., Bennett, D. L., Bril, V., Russell, J.W., Viswanathan, V., 2019. Diabetic neuropathy. Nat. Rev. Dis. Prim. 5, 41. https://doi.org/10.1038/s41572-019-0097-9.

Fernández-Sánchez, L., Lax, P., Campello, L., Pinilla, I., Cuenca, N., 2015. Astrocytes and Müller cell alterations during retinal degeneration in a transgenic rat model of retinitis pigmentosa. Front. Cell. Neurosci. 9, 484. https://doi.org/10.3389/fncel.2015.00484.

Gross, J.G., Glassman, A.R., Liu, D., Sun, J.K., Antoszyk, A.N., Baker, C.W., Bressler, N. M., Elman, M.J., Ferris, F.L. 3rd, Gardner, T.W., Jampol, L.M., Martin, D.F., Melia, M., Stockdale, C.R., Beck, R.W., 2018. Diabetic retinopathy clinical research network. Five-year outcomes of panretinal photocoagulation vs intravitreous ranibizumab for proliferative diabetic retinopathy: a randomized clinical trial. JAMA. Ophthalmol. 136, 1138–1148. https://doi.org/10.1001/jamaophthalmol.2018.3255.

Hageman, G.S., Johnson, L.V., 1986. Biochemical characterization of the major peanut-agglutinin-binding glycoproteins in vertebrate retinae. J. Comp. Neurol. 249, 499–510. https://doi.org/10.1002/cne.902490406.

Hajdú, R., Laurik, L.K., Szabó, K., Dékány, B., Almási, Z., Énzsöly, A., Szabó, A., Radovits, T., Mátyás, C., Oláh, A., Szél, Á., Somfai, G.M., Dávid, C., Lukáts, Á., 2019. Detailed evaluation of possible ganglion cell loss in the retina of zucker diabetic fatty (ZDF) rats. Sci. Rep. 9, 10463 https://doi.org/10.1038/s41598-019-46879-1.

Hammes, H.P., 2005. Pericytes and the pathogenesis of diabetic retinopathy. Horm. Metab. Res. 37, 39–43. https://doi.org/10.1055/s-2005-861361.

Hammoum, I., Benlarbi, M., Dellaa, A., Szabó, K., Dékány, B., Dávid, C., Almási, Z., Hajdú, R.I., Azaiz, R., Charfeddine, R., Lukáts, Á., Ben Chaouacha-Chekir, R., 2017. Study of retinal neurodegeneration and maculopathy in diabetic *Meriones shawi*: a particular animal model with human-like macula. J. Comp. Neurol. 525, 2890–2914. https://doi.org/10.1002/cne.24245.

International Diabetes Federation, 2022. IDF diabetes Atlas, 10th edition. http://www.diabetesatlas.org.

Iribarne, M., Masai, I., 2017. Neurotoxicity of cGMP in the vertebrate retina: from the initial research on rd mutant mice to zebrafish genetic approaches. J. Neurogenet. 31, 88–101. https://doi.org/10.1080/01677063.2017.1358268.

Kalloniatis, M., Nivison-Smith, L., Chua, J., Acosta, M.L., Fletcher, E.L., 2016. Using the rd1 mouse to understand functional and anatomical retinal remodelling and treatment implications in retinitis pigmentosa: a review. Exp. Eye Res. 150, 106–121. https://doi.org/10.1016/j.exer.2015.10.019.

Kang, Q., Yang, C., 2020. Oxidative stress and diabetic retinopathy: molecular mechanisms, pathogenetic role and therapeutic implications. Redox Biol. 37, 101799 https://doi.org/10.1016/j.redox.2020.101799.

Kinuthia, U.M., Wolf, A., Langmann, T., 2020. Microglia and inflammatory responses in diabetic retinopathy. Front. Immunol. 11, 56407710 https://doi.org/10.3389/fimmu.2020.564077, 3389.

Korkmaz-Icöz, S., Radovits, T., Szabó, G., 2018. Targeting phosphodiesterase 5 as a therapeutic option against myocardial ischaemia/reperfusion injury and for treating heart failure. Br. J. Pharmacol. 175, 223–231. https://doi.org/10.1111/bph.13749.

Lieth, E., Barber, A.J., Xu, B., Dice, C., Ratz, M.J., Tanase, D., Strother, J.M., 1998. Glial reactivity and impaired glutamate metabolism in short-term experimental diabetic retinopathy. Penn State Retina Research Group. Diabetes 47, 815–820. https://doi.org/10.2337/diabetes.47.5.815.

Lorenzi, M., 2007. The polyol pathway as a mechanism for diabetic retinopathy: attractive, elusive, and resilient. Exp. Diabetes Res. 2007, 61038 https://doi.org/10.1155/2007/61038.

Maberley, D., Cui, J.Z., Matsubara, J.A., 2006. Vitreous leptin levels in retinal disease. Eye 20, 801–804. https://doi.org/10.1038/sj.eye.6702011.

Marmor, M.F., Kessler, R., 1999. Sildenafil (viagra) and Ophthalmology. Surv. Ophthalmol. 44, 153–162. https://doi.org/10.1016/s0039-6257(99)00079-x.

Mátyás, C., Németh, B.T., Oláh, A., Hidi, L., Birtalan, E., Kellermayer, D., Ruppert, M., Korkmaz-Icöz, S., Kökény, G., Horváth, E.M., Szabó, G., Merkely, B., Radovits, T., 2015. The soluble guanylate cyclase activator cinaciguat prevents cardiac dysfunction in a rat model of type-1 diabetes mellitus. Cardiovasc. Diabetol. 14, 145. https://doi.org/10.1186/s12933-015-0309-x.

Mátyás, C., Németh, B.T., Oláh, A., Török, M., Ruppert, M., Kellermayer, D., Barta, B.A., Szabó, G., Kökény, G., Horváth, E.M., Bódi, B., Papp, Z., Merkely, B., Radovits, T., 2017. Prevention of the development of heart failure with preserved ejection fraction by the phosphodiesterase-5A inhibitor vardenafil in rats with type 2 diabetes. Eur. J. Heart Fail. 19, 326–336. https://doi.org/10.1002/ejhf.711.

Mátyás, C., Kovács, A., Németh, B.T., Oláh, A., Braun, Sz, Tokodi, M., Barta, B.A., Benke, K., Ruppert, M., Lakatos, K.B., Merkely, B., Radovits, T., 2018. Comparison of speckle-tracking echocardiography with invasive hemodynamics for the detection of characteristic cardiac dysfunction in type-1 and type-2 diabetic rat models. Cardiovasc. Diabetol. 17, 13. https://doi.org/10.1186/s12933-017-0645-0.

McGill, T., Cottam, B., Lu, B., Wang, S., Girman, S., Tian, C., Huhn, S.L., Lund, R.D., Capela, A., 2012. Transplantation of human central nervous system stem cells – neuroprotection in retinal degeneration. Eur. J. Neurosci. 35, 468–477. https://doi.org/10.1111/j.1460-9568.2011.07970.x.

Ng, L., Lu, A., Swaroop, A., Sharlin, D.S., Swaroop, A., Forrest, D., 2011. Two transcription factors can direct three photoreceptor outcomes from rod precursor cells in mouse retinal development. J. Neurosci. 31, 11118–111125. https://doi.org/10.1523/JNEUROSCI.1709-11.2011.

Oshitari, T., 2021. Neurovascular impairment and therapeutic strategies in diabetic retinopathy. Int. J. Environ. Res. Publ. Health 19, 439, 10.3390/ijerph19010439.

Qi, C., Mao, X., Zhang, Z., Wu, H., 2017. Classification and differential diagnosis of diabetic nephropathy. J. Diabetes Res. 2017, 8637138 https://doi.org/10.1155/2017/8637138.

Radovits, T., Bömicke, T., Kökény, G., Arif, R., Loganathan, S., Kécsán, K., Korkmaz, S., Barnucz, E., Sandner, P., Karck, M., Szabó, G., 2009. The phosphodiesterase-5 inhibitor vardenafil improves cardiovascular dysfunction in experimental diabetes mellitus. Br. J. Pharmacol. 156, 909–919. https://doi.org/10.1111/j.1476-5381.2008.00098.x.

Ramadan, G.A., 2007. Sorbitol-induced diabetic-like retinal lesions in rats: microscopic study. Am. J. Pharmacol. Toxicol. 2, 89–97. https://doi.org/10.3844/ajptsp.2007.89.97.

Rodríguez, M.L., Pérez, S., Mena-Mollá, S., Desco, M.C., Ortega, Á.L., 2019. Oxidative stress and microvascular alteration in diabetic retinopathy: future therapies. Oxid. Med. Cell. Longev. 2019, 4940825 https://doi.org/10.1155/2019/4940825.

Roessler, G., Vobig, M., Walter, P., Mazinani, B.A., 2019. Ocular side effects of Levitra ® (vardenafil) – results of a double-blind crossover study in healthy male subjects. Drug Des. Dev. Ther. 13, 37–43. https://doi.org/10.2147/DDDT.S186633.

Roger, J.E., Ranganath, K., Zhao, L., Cojocaru, R.I., Brooks, M., Gotoh, N., Veleri, S., Hiriyanna, A., Rachel, R.A., Campos, M.M., Fariss, R.N., Wong, W.T., Swaroop, A., 2012. Preservation of cone photoreceptors after a rapid yet transient degeneration and remodeling in cone-only Nrl-/- mouse retina. J. Neurosci. 32, 528–541. https://doi.org/10.1523/JNEUROSCI.3591-11.2012.

Röhlich, P., Szél, Á., 1993. Binding sites of photoreceptor-specific antibodies COS-1, OS-2 and AO. Curr. Eye Res. 12, 935–944. https://doi.org/10.3109/02713689309020400.

Salama, A., Mostafa, R.E., Omara, E.A., 2018. Effects of phosphodiestrase type 5 inhibitors in epinephrine-induced arrhythmia in rats: involvement of lactate dehydrogenase and creatine kinase downregulation and adiponectin expression. Hum. Exp. Toxicol. 37, 256–264. https://doi.org/10.1177/0960327117695638.

Sandner, P., Follmann, M., Becker-Pelster, E., Hahn, M.G., Meier, C., Freitas, C., Roessig, L., Stasch, J.P., 2015. Effects of PDE5 inhibitors and sGC stimulators in a rat model of artificial ureteral calculosis. PLoS One 10. https://doi.org/10.1371/journal.pone.0141477, 2015.

Sandner, P., Follmann, M., Becker-Pelster, E., Hahn, M.G., Meier, C., Freitas, C., Roessig, L., Stasch, J.P., 2021. Soluble GC stimulators and activators: past, present and future. Br. J. Pharmacol. https://doi.org/10.1111/bph.15698.

Scolaro, L., Parrino, C., Coroniti, R., Otvos, L. Jr., Surmacz, E., 2013 Oct 3. Exploring leptin antagonism in ophthalmic cell models. PLoS One 8 (10), e76437. https://doi.org/10.1371/journal.pone.0076437.

Sharma, Y., Saxena, R.L., Mishra, A., Saxena, A., Natu, S.M., 2012. Advanced glycation end products and diabetic retinopathy. J. Ocul. Biol. Dis. Inform. 5, 63–69. https://doi.org/10.1007/s12177-013-9104-7.

Shin, E.S., Sorenson, M., Sheibani, N., 2014. Diabetes and retinal vascular dysfunction. J. Ophthalmic Vis. Res. 9, 362–373. https://doi.org/10.4103/2008-322X.143378.

Starr, R.C., Nyankerh, C.N.A., Qi, X., Hu, Y., Gorbatyuk, O.S., Sonenberg, N., Boulton, M. E., Gorbatyuk, M.S., 2019. Role of translational attenuation in inherited retinal degeneration. Invest. Ophthalmol. Vis. Sci. 60, 4849–4857. https://doi.org/10.1167/iovs.19-27512.

Stasch, J.P., Pacher, P., Evgenov, O.V., 2011. Soluble guanylate cyclase as an emerging therapeutic target in cardiopulmonary disease. Circulation 123, 2263–2273. https://doi.org/10.1161/CIRCULATIONAHA.110.981738.

Strain, W.D., Paldánius, P.M., 2018. Diabetes, cardiovascular disease and microcirculation. Cardiovasc. Diabetol. 17, 57. https://doi.org/10.1186/s12933-018-0703-2.

Strauss, O., 2005. Retinal pigment epithelium in visual function. Physiol. Rev. 85, 845–881. https://doi.org/10.1152/physrev.00021.2004.

Suganami, E., Takagi, H., Ohashi, H., Suzuma, K., Suzuma, I., Oh, H., Watanabe, D., Ojima, T., Suganami, T., Fujio, Y., Nakao, K., Ogawa, Y., Yoshimura, N., 2004. Leptin stimulates ischemia-induced retinal neovascularization: possible role of vascular endothelial growth factor expressed in retinal endothelial cells. Diabetes 53, 2443–2448. https://doi.org/10.2337/diabetes.53.9.2443. PMID: 15331557.

Susaki, K., Kaneko, J., Yamano, Y., Nakamura, K., Inami, W., Yoshikawa, T., Ozawa, Y., Shibata, S., Matsuzaki, O., Okano, H., Chiba, C., 2009. Musashi-1, an RNA-binding protein, is indispensable for survival of photoreceptors. Exp. Eye Res. 88, 347–355. https://doi.org/10.1016/j.exer.2008.06.019.

Szabó, K., Énzsöly, A., Dékány, B., Szabó, A., Hajdú, R.I., Radovits, T., Mátyás, C., Oláh, A., Laurik, L., Somfai, G.M., Merkely, B., Szél, Á., Lukáts, Á., 2017. Histological evaluation of diabetic neurodegeneration in the retina of Zucker Diabetic Fatty (ZDF) rats. Sci. Rep. 7, 8891. https://doi.org/10.1038/s41598-017-09068-6.

Tomlinson, D.R., Gardiner, N.J., 2008. Glucose neurotoxicity. Nat. Rev. Neurosci. 9, 36–45. https://doi.org/10.1038/nrn2294.

van Aart, C.J.C., Michels, N., Sioen, I., De Decker, A., Nawrot, T.S., De Henauw, S., 2018. Associations of leptin, insulin and lipids with retinal microvasculature in children and adolescents. J. Pediatr. Endocrinol. Metab. 31, 143–150. https://doi.org/10.1515/jpem-2017-0374.

Veres, G., Hagenhoff, M., Schmidt, H., Radovits, T., Loganathan, S., Bai, Y., Korkmaz-Icöz, S., Brlecic, P., Savour, A.A., Karck, M., Szabó, G., 2018. Targeting phosphodiesterase-5 by vardenafil improves vascular graft function. Eur. J. Vasc. Endovasc. Surg. 56, 256–263. https://doi.org/10.1016/j.ejvs.2018.03.025.

Vielma, A.H., Retamal, M.A., Schmachtenberg, O., 2012. Nitric oxide signaling in the retina: what have we learned in two decades? Brain Res. 1430, 112–125. https://doi.org/10.1016/j.brainres.2011.10.045.

Viigimaa, M., Sachinidis, A., Toumpourleka, M., Koutsampasopoulos, K., Alliksoo, S., Titma, T., 2020. Macrovascular complications of type 2 diabetes mellitus. Curr. Vasc. Pharmacol. 18, 110–116. https://doi.org/10.2174/1570161117666190405165151.

Wang, W., Lo, A.C.Y., 2018. Diabetic retinopathy: patophysiology and treatment. Int. J. Mol. Sci. 19, 1816. https://doi.org/10.3390/ijms19061816.

Wang, B., Chandrasekera, P.C., Pippin, J.J., 2014. Leptin- and leptin receptor-deficient rodent models: relevance for human type 2 diabetes. Curr. Diabetes Rev. 10, 131–145. https://doi.org/10.2174/1573399810666140508121012.

Wang, T., Reingruber, J., Woodruff, M.L., Majumder, A., Camarena, A., Artemyev, N.O., Fain, G.L., Chen, J., 2018. The PDE6 mutation in the rd10 retinal degeneration mouse model causes protein mislocalization and instability and promotes cell death through increased ion influx. J. Biol. Chem. 293, 15332–15346. https://doi.org/10.1074/jbc.RA118.004459.

Wright, W.S., Eshaq, R.S., Lee, M., Kaur, G., Harris, N.R., 2020. Retinal physiology and circulation: effect of diabetes. Compr. Physiol. 10, 933–974. https://doi.org/10.1002/cphy.c190021.

Xie, C., Zhu, H., Chen, S., Wen, Y., Jin, L., Zhang, L., Tong, J., Shen, Y., 2020. Chronic retinal injury induced by white LED light with different correlated color temperatures as determined by microarray analyses of genome-wide expression patterns in mice. J. Photochem. Photobiol., B 10, 111977. https://doi.org/10.1016/j.jphotobiol.2020.111977.

Xu, Q., Qaum, T., Adamis, A.P., 2011. Sensitive blood-retinal barrier breakdown quantitation using Evans blue. Invest. Ophthalmol. Vis. Sci. 42, 789–794.

Zeng, X.X., Ng, Y.K., Ling, E.A., 2000. Neuronal and microglial response in the retina of streptozotocin-induced diabetic rats. Vis. Neurosci. 17, 463–471. https://doi.org/10.1017/s0952523800173122.

Zhang, X., Feng, Q., Cote, R.H., 2005. Efficacy and selectivity of phosphodiesterase-targeted drugs in inhibiting photoreceptor phosphodiesterase (PDE6) in retinal photoreceptors. Comparative Study. Invest. Ophthalmol. Vis. Sci. 46, 3060–3066. https://doi.org/10.1167/iovs.05-0257.